A method for calculating inlet distortion effects on stability of split-flow fans

[†]H. Khaleghi [‡]G. Doulgeris [†]M. Boroomand [‡]P. Pilidis [†]A. M. Tousi
khaleghi@aut.ac.ir p.pilidis@cranfield.ac.uk

[†]Aerospace Engineering Department
Amirkabir University of Technology
Tehran, Iran

[‡]Department of Power and Propulsion
School of Engineering
Cranfield University
Cranfield, UK

This paper presents a methodology for calculating the operability and performance of split-flow fans with inlet distortion. A one-dimensional stage-by-stage model has been developed to include parallel compressor theory. The model is capable of providing a detailed definition of the circumferential and radial flow fields. The low-pressure fan is divided to three radial divisions, near-hub, near-tip, and mid-span. The characteristics of each radial segment are calculated by using fan radial profiles. The stable and unstable operations of a split-flow fan, with and without inlet distortion, have been investigated in this study. For the clean inflow surge was triggered by the core compressor, whereas the fan spoiled sector was found to cause the compression system to surge for the distorted case.

NOMENCLATURE

a	speed of sound
A	area
B	Greitzer parameter
BPR	bypass ratio
C_0, C_-, C_+	characteristic lines
CFL	Courant condition
CN	normalised corrected rotor speed $(N/\sqrt{T_{0i}})/(N/\sqrt{T_{0i}})_D$
CM	normalised corrected mass flow rate $(\dot{m}\sqrt{T_{0i}}/P_{0i})/(\dot{m}\sqrt{T_{0i}}/P_{0i})_{ch}$
e	energy
F_f	friction force
F_S	stage force
H	total enthalpy
k	constant
L	effective length
M	Mach number
MOC	method of characteristics
$\dot{m}$	mass flow rate
N	shaft rotational speed
P	static pressure
P_0	total pressure
$\dot{Q}$	rate of heat transfer
t	time
T_0	total temperature
u	axial velocity
U_m	rotor mean velocity
V	volume
$\dot{W}_{shaft}$	rate of shaft work
x	axial direction
γ	specific heat ratio
δ, ε, ζ, η	defined parameters
ρ	density
ϕ	flow coefficient
ψ_P	pressure coefficient
ψ_T	temperature coefficient

Paper No. 3266. Manuscript received 10 December 2007, accepted 22 June 2009.

https://doi.org/10.1017/S0001924000003250 Published online by Cambridge University Press

Subscripts

amb	ambient
b	bleed
c	compressor
ch	choking condition
D	design point
e	exit
i	inlet

1.0 INTRODUCTION

Adequate stability is an important feature of any compression system design. The peak operating point, where compressors deliver the most compression, is on the boundary of stability. At this operating point, disturbances such as engine acceleration and inlet distortion are capable of destabilising the compressor by triggering surge or rotating stall phenomena. Surge is characterised by large amplitude oscillations in the annulus-averaged flow through the compression system. In rotating stall, however, one finds one or more regions of stalled flow that rotate around the compressor annulus[1-3]. In order to simulate post-stall behavior of compressors, one-dimensional and two-dimensional models have been developed by a number of researchers[4-8]. One-dimensional models are commonly stage-by-stage, whereas two-dimensional approaches are generally based on Moore-Greitzer model. More recently, a blockage-mixing based model capable of calculating moderate to long length-scale instabilities within a compression system has been developed by Longley[9]. Inlet flow distortions reduce performance and stability of a compression system. Although the inlet distortions encountered are generally three-dimensional, they are commonly divided to radial and circumferential non-uniformities, which are separately modeled in order to simplify the simulations. Radial distortions can be treated by methods that assume axisymmetric inlet flows, whereas parallel compressor theory is the basic approach to circumferential distortion. Series of experiments were undertaken by Reid[10] to investigate the effects of different radial and circumferential distortion patterns on compressor performance. Results indicated the existence of a critical sector angle for circumferential distortions, above which there is little change in the exit static pressure[10,11]. The critical sector of spoiling is found to be between about 60 and 90 deg, as illustrated in Fig. 1. A number of researchers used one-dimensional models, by employing parallel compressor theory, to study the impact of inlet distortion on compressor stability and performance (e.g., Longley and Greitzer[11], Korn[12], Steenken[13], Mazzawy[14], Kimzey[15], Hale and Davis[16], and Shahrokhi and Davis[17]). In the work done by Mazzawy[14], a detailed definition of the circumferential flow field was presented by employing multiple parallel segments. Billet *et al*[18] reported an alternative approach to parallel compressor theory which permits direct interaction of radial and circumferential control volumes via Euler equations, including body forces associated with a blade row. Hale *et al*[19] used the Billet concept to simulate both radial and circumferential distortion patterns. Xu *et al*[20] proposed a three-dimensional CFD method, using viscous body force terms, which is capable of simulating inlet distortions. A three-dimensional unsteady code, based on Euler equations, has been developed by Chima[21] in order to investigate distortion and stall phenomena in axial compressors. Blade row turning, losses, and deviation were modeled by using body force terms, and a separate Navier-Stokes turbomachinery code was employed to calculate the body force input data at one operating point near stall. Although several studies have been performed on modeling of inlet distortion, few works have been reported on inlet distortion effects on the performance of split-flow fans, while exhibiting a detailed definition of the circumferential and radial flow fields.

The objective of the current study is to develop a model for calculating inlet distortion effects on stability of high BPR fans, where the radial variation of properties is pronounced. For this purpose, a stage-by-stage model[6] has been developed to include parallel compressor theory, and the operability and performance of a split-flow fan have been studied, with and without inlet distortion.

2.0 GEOMETRY

Figure 2 shows the geometry of the split-flow fan studied in this work. The fan splits into a bypass duct and an axial flow compressor. The core compressor consists of an inlet guide vane (IGV) followed by four stages. The internal ducts are also shown in this figure. The bypass and core flows discharge into two separate plenum chambers with constant volumes.

3.0 MODELING TECHNIQUE

3.1 Parallel compressor

Parallel compressor is a one dimensional approach to inlet distortion. It was demonstrated by Doyle and Horlock[22] that this theory is a reliable method for preliminary prediction of the effects of circumferential distortions on compressor performance. In the parallel compressor concept, shown in Fig. 3, the compressor is divided into

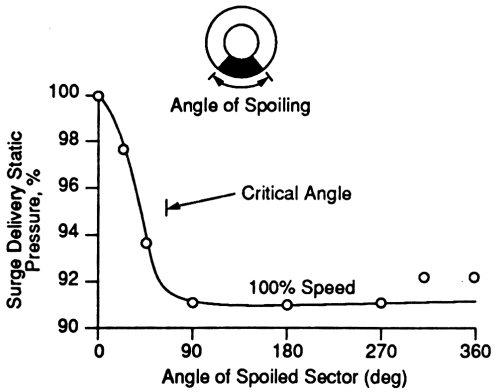


Figure 1. Effect of distorted sector width[10].

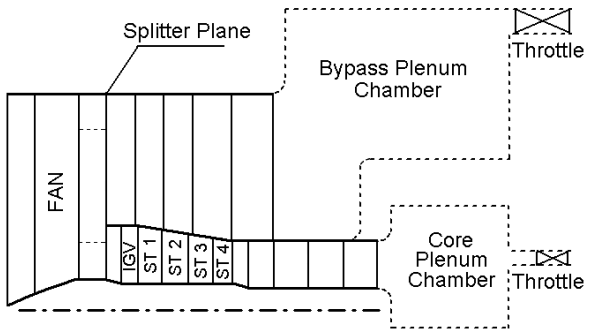


Figure 2. Geometry of the compression system.

https://doi.org/10.1017/S0001924000003250 Published online by Cambridge University Press

some equal-area segments. Each region is then treated as a separate compressor with individual inlet boundary condition. However, the exit boundary condition is common for all of the divisions and is the uniformity of back static pressure. In the basic parallel compressor model, it is assumed that the compressor characteristic in each division is identical to that obtained with uniform inflow. It is also assumed that the circumferential cross flow within the compressor is negligible. The stability criterion for the basic parallel compressor theory is the attainment of the uniform inlet stall flow in one of the distorted sectors, which in known to be inadequate for accurate prediction of stall point[14]. In the current study the near-stall condition is judged to be the last stable operating point prior to large oscillations in the flow parameters of a single segment, which characterise surge. The near-stall point is then obtained from the average pressure ratio and the total mass flow rate from all of the segments.

Some approaches have been taken by a number of researchers in order to improve the prediction of stall point with parallel compressor model: Empirical correlation of the loss in stall margin[11,23] and extension of the model to include fluid dynamic effects (i.e., mass redistribution) and non-steady flow phenomena associated with rotor blades passing through non-uniform flow[14,15,17]. The current study does not include such modifications, because the main objective was to implement the parallel compressor model for calculating the effects of inlet distortion on stability and performance of high BPR fans. In the current work the fan is divided to three radial segments: Near-hub, near-tip, and mid-span. In the circumferential direction, however, each radial segment is divided to a user-defined number of equal-area parts (eight segments for the current configuration). Figure 4 illustrates the parallel compressors in different radial divisions of the fan.

3.2 Governing equations and numerical scheme

The unsteady Euler equations, including turbomachinery and friction source terms, are used as the governing equations in this study:

Continuity:

$$\frac{\partial \rho}{\partial t}+\frac{\partial}{\partial x}(\rho u)=-\rho u\frac{\mathrm{d}(\ln A)}{\mathrm{d}x}-\frac{\mathrm{d}\dot{m}_b}{A\mathrm{d}x} \quad \ldots (1)$$

Momentum:

$$\frac{\partial}{\partial t}(\rho u)+\frac{\partial}{\partial x}(\rho u^2+P)= -\frac{\rho u^2}{A}\frac{\mathrm{d}A}{\mathrm{d}x}+\frac{F_S}{A\mathrm{d}x}-\frac{F_f}{A\mathrm{d}x}-\frac{\mathrm{d}\dot{m}_b u_{bx}}{A\mathrm{d}x} \quad \ldots (2)$$

Energy:

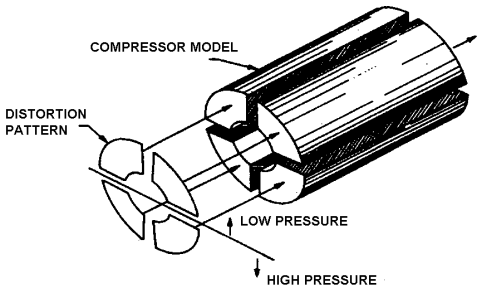
$$\frac{\partial}{\partial t}(\rho e)+\frac{\partial}{\partial x}(\rho u e+Pu)=\frac{\dot{Q}}{A\mathrm{d}x}-\frac{\dot{W}_{shaft}}{A\mathrm{d}x} -\frac{\rho u}{A}\left(\frac{u^2}{2}+\frac{\gamma}{\gamma-1}\frac{P}{\rho}\right)\frac{\mathrm{d}A}{\mathrm{d}x}-(e_b+P/\rho)\frac{\mathrm{d}\dot{m}_b}{A\mathrm{d}x} \quad \ldots (3)$$

Method of characteristics (MOC) has been employed as the numerical scheme to solve the governing equations. Based on MOC, the partial differential equations given in Equations (1) to (3) reduce to ordinary differential equations along the characteristic lines (C_0, C_+, and C_-). The resultant equations are often called the 'characteristic compatibility relations'. The expressions for the characteristic lines and compatibility relations are as follows:

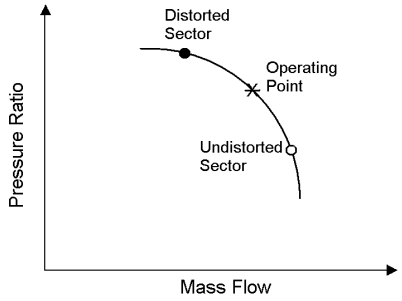
Characteristic and compatibility of C_0:

$$\mathrm{d}x/\mathrm{d}t = u \quad \ldots (4)$$

$$\frac{\mathrm{d}P}{\mathrm{d}t}-a^2\frac{\mathrm{d}\rho}{\mathrm{d}t}=\eta \quad \ldots (5)$$



a) General concept



b) Operating point analysis

Figure 3. Parallel compressor model.

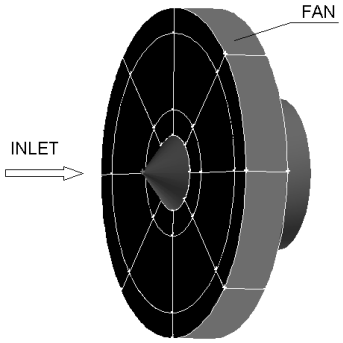
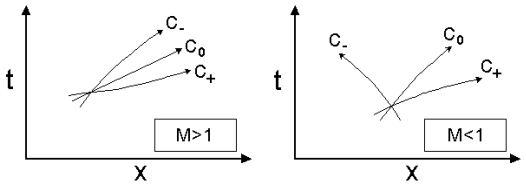
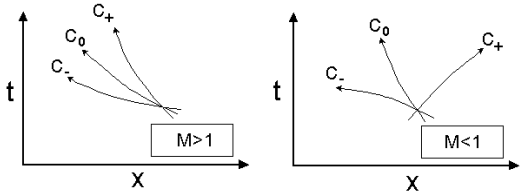


Figure 4. Parallel compressors in three radial divisions.



a) Forward flow



b) Backward flow

Figure 5. Configurations of the characteristic lines.

https://doi.org/10.1017/S0001924000003250 Published online by Cambridge University Press

Characteristic and compatibility of C_+:

$$dx/dt = u + a \quad \ldots (6)$$

$$\frac{du}{dt} + \frac{1}{\rho a}\frac{dP}{dt} = \frac{1}{\rho a}\left(a^2\varepsilon + a\delta + \eta\right) \quad \ldots (7)$$

Characteristic and compatibility of C_-:

$$dx/dt = u - a \quad \ldots (8)$$

$$\frac{du}{dt} - \frac{1}{\rho a}\frac{dP}{dt} = \left(\frac{-1}{\rho a}\right)\left(a^2\varepsilon - a\delta + \eta\right) \quad \ldots (9)$$

Where:

$$\varepsilon = -\rho u\frac{d(\ln A)}{dx} - \frac{d\dot{m}_b}{Adx} \quad \ldots (10)$$

$$\delta = \frac{F_S}{Adx} - \frac{F_f}{Adx} - \frac{d\dot{m}_b}{Adx}\left(u_{bx} - u\right) \quad \ldots (11)$$

$$\eta = (\gamma - 1)[\zeta - u\delta] \quad \ldots (12)$$

$$\zeta = \frac{\dot{Q}}{Adx} - \frac{\dot{W}_{shaft}}{Adx} - \frac{d\dot{m}_b}{Adx}\left(H_b - H\right) \quad \ldots (13)$$

The characteristic lines might have different configurations depending on the direction and Mach number of the flow. Figure 5 illustrates all of the possible configurations for the characteristic lines. The compatibility relations (Equations (5), (7) and (9)) should be solved along the characteristic lines by marching in time. Stability criterion must be set since the code is explicit. Therefore, the Courant condition (CFL) is satisfied by using a variable time step which is expressed in Equation (14). The minimum value of 'k' in Equation (14) is 1. However, in the current work 'k' is chosen to be 0·25.

$$\Delta t_{\min} = \frac{k(\Delta x_{\min})}{(|u| + a)_{\max}} \quad \ldots (14)$$

3.3 Component characteristics

To provide stage force and shaft work for the momentum and energy equations, a set of quasi-steady stage characteristics must be available for closure. The stage characteristics provide the pressure and temperature variation across each stage as a function of steady airflow[4]. For rotating stall and surge simulations, the compressor characteristic is required to be defined beyond the surge point. It is difficult to obtain this part of operation by experiments. However, from an understanding of how a surge cycle is formed assessment can be made of the complete characteristic shape[3,16,24]. The pressure and temperature characteristics used in the present study have the typical form of Fig. 6[16]. The flow, pressure, and temperature coefficients are defined as follows:

$$\phi = \frac{\dot{m}\sqrt{T_{0i}/T_{amb}}}{P_{0i}/P_{amb}}\frac{\left(N/\sqrt{T_{0i}}\right)_D}{\left(N/\sqrt{T_{0i}}\right)} \quad \ldots (15)$$

$$\psi_T = \frac{T_{0e} - T_{0i}}{T_{0i}}\left(\frac{\left(N/\sqrt{T_{0i}}\right)_D}{\left(N/\sqrt{T_{0i}}\right)}\right)^2 \quad \ldots (16)$$

$$\psi_P = \frac{P_e - P_i}{P_i}\left(\frac{\left(N/\sqrt{T_{0i}}\right)_D}{\left(N/\sqrt{T_{0i}}\right)}\right)^2 \quad \ldots (17)$$

It is well known that high BPR fans have pronounced aerodynamic profiles in the radial direction. The profile of properties at the outlet of the fan is independent of how the flow is split downstream, as described by Marshall[25]. Yin *et al*[26] generated some notional radial profiles of fan performance that were realistic but do not apply to any particular fan. Similar profiles were used in this study. An averaging technique similar to that used by Yin *et al*[26] was then employed in order to generate the pressure and temperature characteristics of each radial segment for one speed line. The characteristics of each radial division have been extended to unstable operation, similar to the core compressor stages.

3.4 Boundary conditions

The following boundary conditions are used in the current work: At the inlet boundary, the total pressure and total temperature are specified during normal forward flow. During reverse flow, which may occur in deep surge cycle, the inlet is converted to an outlet boundary with the ambient static pressure specified. A transient boundary condition is used at the outlet. As stated earlier, it is assumed in this study that the core and bypass flows discharge into separate plenum chambers having constant volumes. By assuming isentropic gas law and using the conservation of mass through the plenum, it can be shown that the pressure in the plenum varies as[1,27]:

$$\frac{dP_{plenum}}{dt} = \frac{a^2{}_{plenum}}{V_{plenum}}\left(\dot{m}_{plenum} - \dot{m}_{throttle}\right) \quad \ldots (18)$$

In the above equation, $\dot{m}_{plenum}$ represents the computed mass flow rate at the core or bypass exit planes, whereas $\dot{m}_{\text{throttle}}$ is the desired mass flow rate. In addition, a_{plenum} and V_{plenum} are the speed of sound calculated at the core and bypass exit planes and the volume of the plenum chamber, respectively. A first order discretisation of Equation (18) is used in order to specify the back pressure at the core and bypass outlet boundaries during each numerical time step. Greitzer[1] introduced a parameter, given in Equation (19), which determines whether a given compressor exhibits surge or rotating stall. He found a critical value for B bellow which the result of instability is in the form of rotating stall, whereas for greater values the mode of instability is the large amplitude oscillations that characterise surge. This critical value for B was found to be 0·8. In the current study B greater than 0·8 is preferred because one-dimensional modeling is more similar to surge nature, as compared to rotating stall. Therefore, the volumes of the core and bypass plenums were set to 2 and 10m^3 respectively, causing B to be greater than 0·8 for the fan and core compressor. The stable operation of the compression system is not influenced by the volumes of the plenum chambers, whereas the surge cycle frequency would vary by changing these volumes (i.e., greater volume-lower frequency).

$$B = \left(U_m/2a\right)\sqrt{V_{plenum}/(A_c L_c)} \quad \ldots (19)$$

Additional relations are required at the splitter plane for closure[16]. At the fan exit plane static pressure is specified. The radial variation in exit static pressure relative to the average is input, whereas the average level of static pressure required to satisfy the desired total mass flow is determined iteratively. At the inlet of the core and bypass ducts the total pressure and total temperature are imposed, which are calculated based on area averaging at the splitter plane. It should be noted that the outer diameter of the core compressor inlet is greater than that of the fan near-hub segment at the splitter plane. These conditions are shown in Fig. 7. It is assumed in this study that the BPR remains constant at the stable operating conditions from choke to near-stall. Furthermore, the physical shaft speeds of both the fan and core compressor are kept constant.

https://doi.org/10.1017/S0001924000003250 Published online by Cambridge University Press

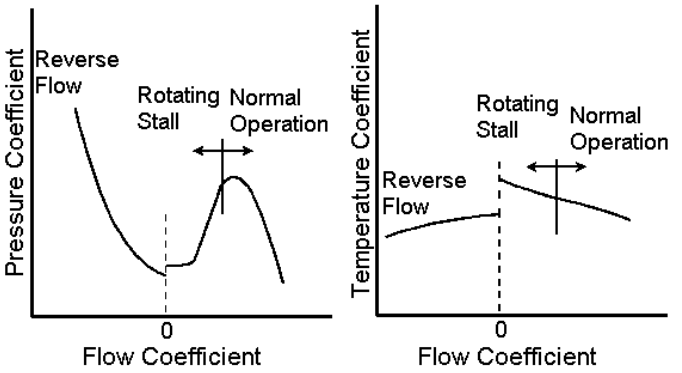


Figure 6. Typical stage characteristics.

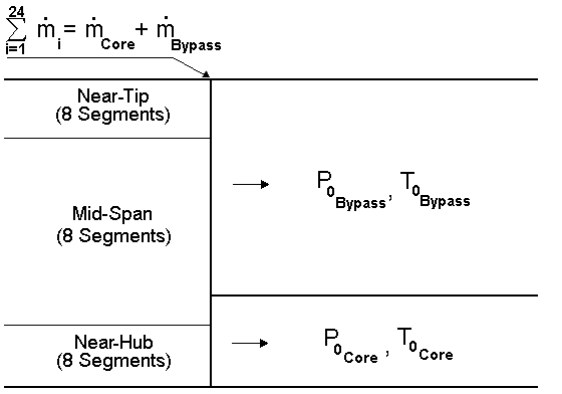


Figure 7. Additional conditions at the splitter plane.

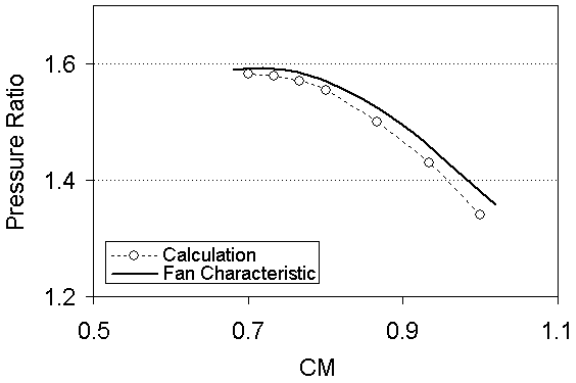
4.0 RESULTS AND DISCUSSION

4.1 Separate component configurations

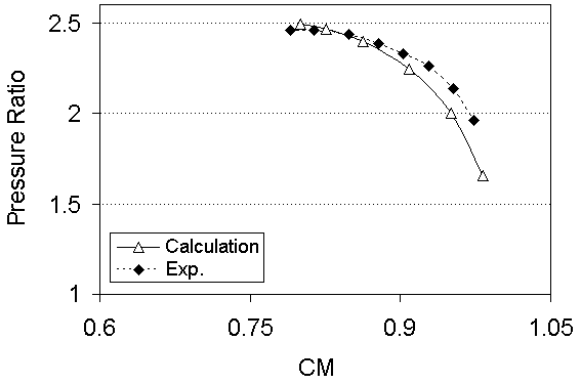
In the current study, the fan and core compressor were modeled separately first. For each component, the physical shaft speed was kept constant and the ambient conditions were used at the inlet. Furthermore, the same ducting shown in Fig. 2 was used downstream of each case. The stable operating points were calculated by time marching. Calculations were performed from choke to stall, by gradually decreasing the throttle mass flow rate (Equation (18)). The corresponding choking mass flow of each case was used to normalise the corrected mass flows. In Fig. 8(a), the calculated characteristic of the separate fan is compared to the fan characteristic obtained from the fan radial profiles. This figure shows relatively good agreement between the two characteristics. A comparison between the experimental data and the calculated characteristic of the separate compressor, at *CN* equivalent to 0·8, is presented in Fig. 8(b). As illustrated, the compressor characteristic is calculated with reasonable accuracy. Figure 9 depicts the radial profile of fan pressure ratio at *CM* equivalent to 0·8. The calculated pressure ratios of the radial divisions are also shown in this plot. As shown, the computed average values of fan pressure ratio in each radial division agree fairly well with the fan profile.

4.2 Clean inflow

The computations were performed for the split-flow fan with clean inflow and BPR equivalent to five. Throttling is achieved by decreasing the desired mass flow rate. As stated earlier, the near-stall point is judged to be the last stable operating point prior to large oscillations in the flow parameters of a single segment, which characterise surge. The overall characteristics of the fan and core compressor are presented in Fig. 10. The mass flows are corrected and normalised by using the corresponding choking mass flow of the separate configuration. The fan pressure ratios are calculated by mass averaging the total pressures along the span. As shown in Fig. 10(a), the low-pressure fan follows the same characteristic of the separate configuration. Figure 10(b) shows a reduction in the normalised corrected speed (*CN*) of the core compressor, when compared to the separate configuration. The physical rotational speed of the compressor is kept constant in this work. Thus, the increase in the compressor inlet total temperature lowers the corrected speed. A set of simulations was also carried out for the separate compressor configuration by applying the fan exit total pressure and temperature, at each operating point, as the inlet boundary of the core compressor. Identical changes in the normalised corrected speed were observed. Figure 10 shows that the last operating point is away from the fan surge point, whereas it is



a) Separate fan



b) Separate compressor

Figure 8. Component characteristics.

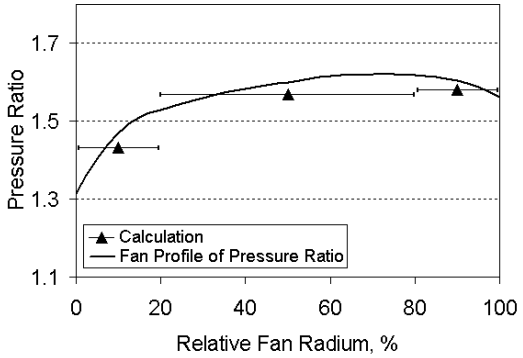
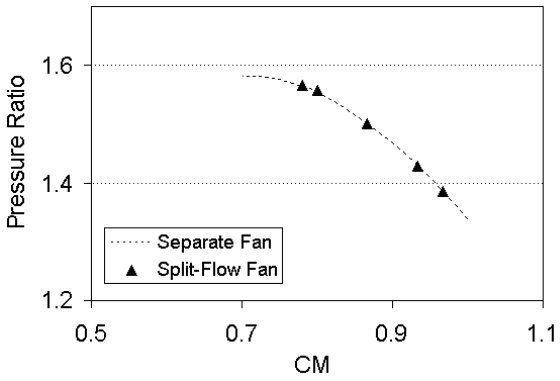
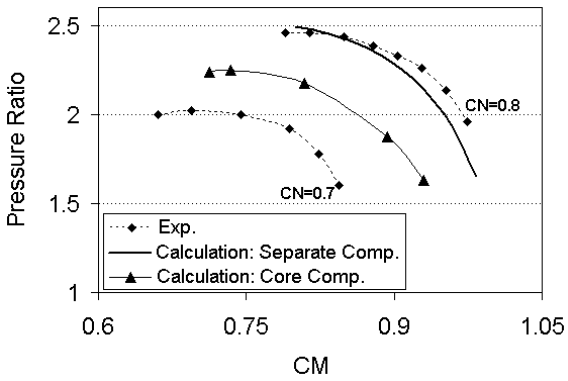


Figure 9. Radial profile of fan pressure ratio at CM equivalent to 0·8.

https://doi.org/10.1017/S0001924000003250 Published online by Cambridge University Press



a) Fan



b) Core compressor

Figure 10. Calculated characteristics for the clean inflow.

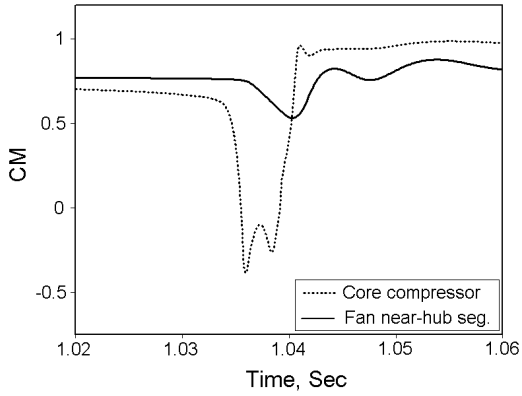
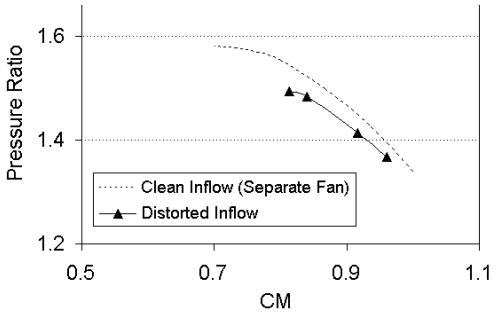
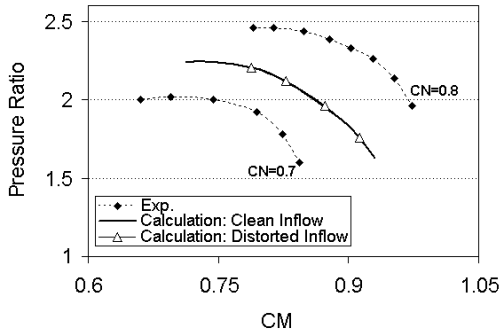


Figure 11. Time traces of CM for the clean inflow.



a) Fan



b) Core compressor

Figure 12. Calculated characteristics for the distorted inflow.

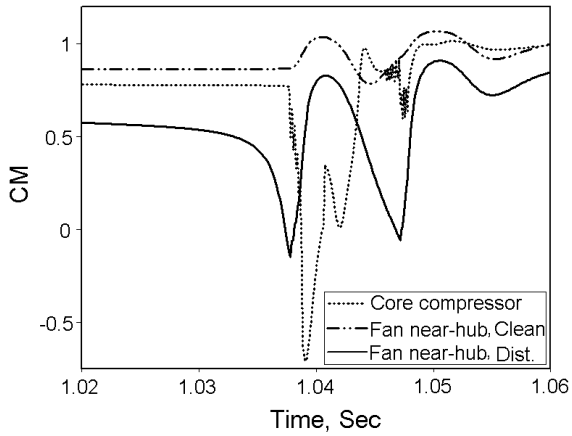


Figure 13. Time traces of CM for the distorted inflow.

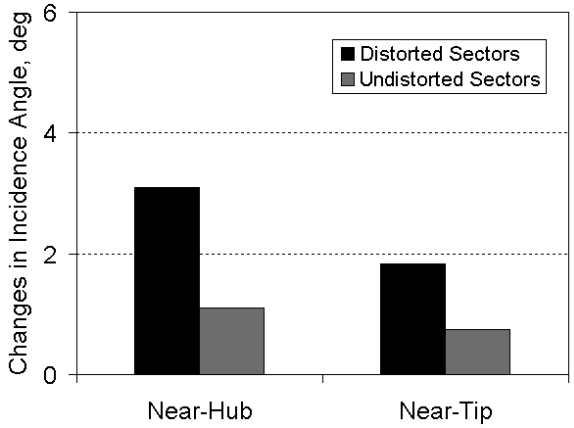


Figure 14. Changes in incidence angle of the near-hub and near-tip segments for the distorted inflow.

https://doi.org/10.1017/S0001924000003250 Published online by Cambridge University Press

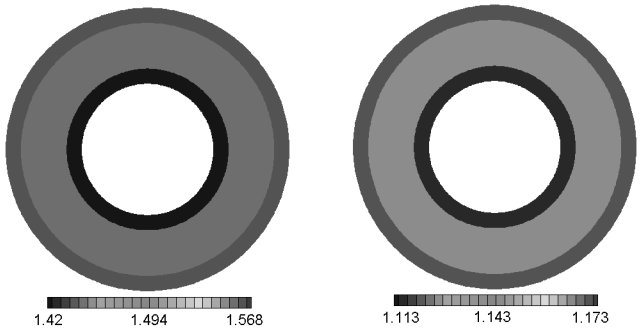
close to the stability limit of the core compressor. It is concluded that surge is triggered by the core compressor. The transient response of the components during the inception of instabilities can assist to support this finding. In order to initiate the instabilities, the total mass flow was decreased by about 0·4 percent at the last stable operating point. Figure 11 shows the time traces of the normalised corrected mass flow at the inlet of the fan near-hub segment and core compressor. The compression system has been throttled at the time equivalent to one Second. As shown in Fig. 11, surge is initiated by the core compressor. The deep surge triggered by the high-pressure compressor results in the flow oscillations at the fan inlet plane.

4.3 Distorted inflow

In order to study the effect of inlet distortion on the stability of the current compression system, a 10 percent total pressure distortion in the circumferential direction was applied to the fan inlet plane. The width of the spoiled sector was chosen to be 90°deg. The simulations were performed from choke to stall for the BPR equivalent to five, similar to the clean inflow case. The effects of inlet distortion on the characteristics of the fan and core compressor are shown in Figs 12(a) and 12(b), respectively. The mass flows are corrected and normalised by using the corresponding choking mass flow of the separate configuration. The fan characteristic is calculated by circumferentially and radially mass averaging the total pressures at the fan exit. As shown in Fig. 12(b), for the distorted case the last operating point is away from the stability boundary of the core compressor, which suggests that surge is triggered by the fan. Figure 12(a) shows the fan characteristics for the separate configuration with clean inflow and the split-flow fan with inlet distortion. Comparing the fan surge point of the distorted case with that of the clean inflow shows about 16 percent reduction in the corrected mass flow and 5·7 percent drop in the fan pressure ratio.

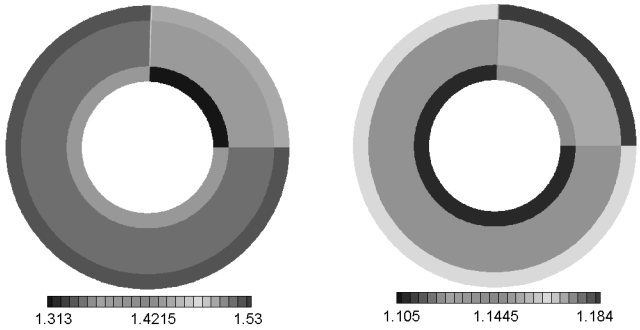
Figure 13 shows the transient response of the core compressor and the fan near-hub segments, during the inception of instabilities, for the distorted inflow case. In order to initiate the instabilities, the total mass flow was decreased by about 0·4 percent at the last stable operating point, similar to the clean inflow case. The compression system has been throttled at the time equivalent to one second. As shown in Fig. 13, surge is initiated by the distorted sector near the hub of the fan. It is also shown that the stalling disturbance of the distorted sector causes the core compressor to deep surge, with the occurrence of reverse flow at its inlet plane. Furthermore, a second stalling disturbance is imposed to the fan by the core compressor. Figure 14 depicts the changes in incidence angle near the hub and tip of the fan. The incidence angle variation was evaluated by differencing the relative flow angles, calculated from the axial and circumferential velocities at the fan inlet and two conditions: The fan surge point and an operating point with about four percent greater corrected mass flow. As seen, the greatest increase in the incidence is due to the spoiled sector near the hub of the fan.

In order to clarify the effect of inlet distortion, contour plots of the fan total pressure and total temperature ratios are presented in Figs 15 and 16, for the clean and distorted cases, respectively. In order to understand the effect of inlet distortion, the results should be compared under the same conditions. This is achieved by comparing the results at the mass flow corresponding to the near-stall condition of the distorted case. Figure 16(a) shows lower pressure ratio within the spoiled sector, when compared with the clean inflow case, Fig. 15(a). In contrast, the temperature ratio of the distorted sector is greater, which is due to unequal work input for this segment. However, the mass-averaged temperature ratios were found to be approximately identical for the clean and distorted cases.



a) Pressure ratio b) Temperature ratio

Figure 15. Contours of pressure and temperature ratios for the clean inflow.



a) Pressure ratio b) Temperature ratio

Figure 16. Contours of pressure and temperature ratios for the distorted inflow.

5.0 CONCLUSION

An algorithm for calculating the operability and performance of split-flow fans has been developed. The stable and unstable operations of a high BPR fan, with and without inlet distortion, were investigated. The following observations and conclusions can be drawn from this work:

1- By using the fan radial profiles of aerodynamic properties, the parallel compressor model can be extended to provide a detailed definition of both radial and circumferential flow fields for high BPR fans with inlet distortion.

2- For the current compression system, surge was initiated by the core compressor with clean inflow, whereas the low-pressure fan was shown to cause the compression system to surge when a 90°deg circumferential distortion was applied. Results also indicated that the stalling disturbance was triggered by the distorted sector near the hub of the fan.

3- Results showed about 16 percent reduction in the corrected mass flow and 5·7 percent drop in the pressure ratio of the fan surge point for the distorted case, when compared to the separate fan configuration with clean inflow.

This paper did not include modifications to the parallel compressor theory (e.g., dynamic blade response and mass redistribution), because the main objective was to develop a model for calculating inlet distortion effects on stability of high BPR fans, where the radial variation of properties is pronounced. These modifications, together with the effects of inlet distortion on the performance of an entire turbofan engine, will be the future investigation of the present authors.

https://doi.org/10.1017/S0001924000003250 Published online by Cambridge University Press

ACKNOWLEDGMENTS

The authors gratefully acknowledge the British Council and Iranian Ministry of Science, Research and Technology for their support.

REFERENCES

1. GREITZER, E.M. Surge and rotating stall in axial flow compressors – part 1: theoretical compression system model and part 2: experimental results and comparison with theory, *J Eng Power*, 1976, **98**, (2), pp 190-217.
2. GREITZER, E.M. Review- Axial compressor stall phenomena, *J Fluids Eng*, 1980, **102**, pp 134-151.
3. DAY, I.J., GREITZER, E.M. and CUMPSTY, N.A. Prediction of compressor performance in rotating stall, *J Eng for Power*, 1978, **100**, pp 1-14.
4. DAVIS JR, M.W. and O'BRIEN, W.F. Stage-by-stage poststall compression system modeling technique, *J Propulsion and power*, 1991, **7**, (6), pp 997-1005.
5. GARRARD, D., DAVIS JR, M., HALE, A., CHALK, J. and SAVELLE, S. Analysis of gas turbine engine operability with the aerodynamic turbine engine code, ISABE 97-7034, 1997.
6. KHALEGHI, H., BOROOMAND, M. and TOUSI, A.M. A stage by stage simulation and performance prediction of gas turbine, AIAA Paper AIAA-2005-1012, 2005.
7. MOORE, F.K. and GREITZER, E.M. A theory of post-stall transients in axial compression systems part 1- development of equations, *J Eng Gas Turbine and Power*, 1986, **108**, pp 68-76.
8. HENDRICKS, G.J., BONNAURE, L.P., LONGLEY, J.P., GREITZER, E.M. and EPSTEIN, A.H. Analysis of rotating stall onset in high speed axial flow compressors, AIAA Paper AIAA-1993-2233, 1993.
9. LONGLEY, J.P. Calculating stall and surge transients, ASME Paper GT2007-27378, 2007.
10. REID, C. The response of axial flow compressors to intake flow distortion, ASME Paper 69-GT-29, 1969.
11. LONGLEY, J.P. and GREITZER, E.M. Inlet distortion effects in aircraft propulsion system integration, AGARD Lecture Series, AGARD-LS-183, 1992.
12. KORN, J.A. Estimated effect of circumferential distortion on axial compressors using parallel compressor theory and dynamic stall delay, AIAA Paper AIAA-1974-233, 1974.
13. STEENKEN, W.G. Modeling compression component stability characteristics – effects of inlet distortion and fan bypass duct disturbances, AGARD-CP-324, 1983.
14. MAZZAWY, R.S. Multiple segment parallel compressor model for circumferential flow distortion, *J Eng Power*, 1977, **99**, pp 288-296.
15. KIMZEY, W.F. An analysis of the influence of some external disturbances on the aerodynamic stability of turbine engine axial flow fans and compressors, AEDC-TR-77-80, 1977.
16. HALE, A.A. and DAVIS Jr., M.W. Dynamic turbine engine compressor code DYNTECC – theory and capabilities, AIAA Paper AIAA-92-3190, 1992.
17. SHAHROKHI, K.A. and DAVIS Jr., M.W. Application of a modified dynamic compression system model to a low aspect ratio fan: effects of inlet distortion, AIAA Paper AIAA-95-0301, 1995.
18. BILLET, G., HUARD, J., CHEVALIER, P. and LAVAL, P. Experimental and numerical study of the response of an axial compressor to distorted inlet flow, *J Fluids Engineering*, 1988, **110**, (4), pp 355-360.
19. HALE, A.A., DAVIS JR, M.W. and KNEILE, K.R. Turbine engine analysis compressor code: TEACC part 1: technical approach and steady results, AIAA Paper AIAA-94-0148, 1994.
20. XU, L., HYNES, T.P. and DENTON, J.D. Towards long length scale unsteady modelling in turbomachines, Proceedings of the Institution of Mechanical Engineers. Part A, *J Power and Energy*, 2003, **217**, pp 75-82.
21. CHIMA, R.V. A three-dimensional unsteady CFD model of compressor stability, ASME Paper GT2006-90040, 2006.
22. DOYLE, M.D.C. and HORLOCK, J.H. Circumferential asymmetry in axial flow compressors, *Aeronaut J* , 1966, **70**, pp 956-957.
23. WILLIAMS, D.D. Review of current knowledge on engine response to distorted inflow conditions, AGARD CP-400, 1986.
24. GAMACHE, R.N. and GREITZER, E.M. Reverse flow in multistage axial compressors, AIAA Paper AIAA-1986-1747, 1986.
25. MARSHALL, C.D. The Modeling of high bypass ratio turbofans, Msc Thesis, School of Mechanical Engineering, Cranfield University, Cranfield, 1998.
26. YIN, J., HALES, R., PILIDIS, P., CURNOCK, B. and MEADS, R. Transient performance for high-bypass ratio turbofan models, *J Aircr Eng and Aerospace Technology*, 2000, **72**, (6), pp 518-523.
27. NIAZI, S., STEIN, A. and SANKAR, L.N. Computational analysis of stall control using bleed valve in a high-speed compressor, AIAA Paper AIAA-2000-3507, 2000.

https://doi.org/10.1017/S0001924000003250 Published online by Cambridge University Press